Untargeted metabolomics approach for unraveling robust biomarkers of nutritional status in fasted gilthead sea bream (*Sparus aurata*)

Ruben Gil-Solsona[1], Jaime Nácher-Mestre[1,2], Leticia Lacalle-Bergeron[1], Juan Vicente Sancho[1], Josep Alvar Calduch-Giner[2], Félix Hernández[1] and Jaume Pérez-Sánchez[2]

[1] Research Institute for Pesticides and Water (IUPA), University Jaume I, Castellón, Spain
[2] Institute of Aquaculture Torre de la Sal (IATS, CSIC), Ribera de Cabanes, Castellón, Spain

ABSTRACT

A metabolomic study has been performed to identify sensitive and robust biomarkers of malnutrition in farmed fish, using gilthead sea bream (*Sparus aurata*) as a model. The metabolomic fingerprinting of serum from fasted fish was assessed by means of ultra-high performance liquid chromatography coupled to quadrupole time-of-flight mass spectrometry. More than 15,000 different *m/z* ions were detected and Partial Least Squares–Discriminant analysis allowed a clear differentiation between the two experimental groups (fed and 10-day fasted fish) with more than 90% of total variance explained by the two first components. The most significant metabolites (up to 45) were elucidated on the basis of their tandem mass spectra with a broad representation of amino acids, oligopeptides, urea cycle metabolites, L-carnitine-related metabolites, glutathione-related metabolites, fatty acids, lysophosphatidic acids, phosphatidylcholines as well as biotin- and noradrenaline-related metabolites. This untargeted approach highlighted important adaptive responses in energy and oxidative metabolism, contributing to identify robust and nutritionally-regulated biomarkers of health and metabolic condition that will serve to assess the welfare status of farmed fish.

INTRODUCTION

Fish aquaculture is the sector of animal livestock production with higher growth rates at the global level. This industry highly contributes to cover the current but also the future demand of nutritious quality food for human consumption (*Ottinger, Clauss & Kuenzer, 2016*). This starts with the selection of high quality raw materials in order to ensure the development of an efficient and environmentally sustainable sector. However, we need to refine our knowledge on nutrient requirements to produce more robust, safe and quality fish, especially with the advent of new diet formulations based on alternative plant ingredients rather than marine feedstuffs (*Karalazos et al., 2007*; *Médale et al., 2013*; *Benedito-Palos et al.,*

Corresponding authors
Juan Vicente Sancho, sanchoj@uji.es
Jaume Pérez-Sánchez,
jaime.perez.sanchez@csic.es

2016). As a result, research in fish nutrition is moving from classical methodologies to omics approaches, including transcriptomics (*Benedito-Palos, Ballester-Lozano & Pérez-Sánchez, 2014*; *Louro, Power & Canario, 2014*), proteomics (*Rodrigues et al., 2012*; *Wrzesinski et al., 2013*) and metabolomics (*Kullgren et al., 2010*; *Silva et al., 2014*; *Asakura et al., 2014*).

Unlike nucleic acid or protein-based omic techniques, metabolomics has to deal with low-molecular weight metabolic entities (<1,000 Da) with diverse chemical and physical properties (*Kell, 2004*), which can vary from millimolar to picomolar concentrations. Two are the main analytical platforms currently used in metabolomics studies: nuclear magnetic resonance (NMR) (*Emwas, 2015*) and mass spectrometry (MS) (*Castro-Puyana & Herrero, 2013*). Most of the studies of metabolomic profiling or fingerprinting of body fluids in livestock animals are based on NMR approaches due to its great robustness and elucidation power (*Kullgren et al., 2010*; *Xu et al., 2015*; *Jégou et al., 2016*; *Niu et al., 2016*), although one of the main drawbacks of this technique is its low sensitivity (*Emwas, 2015*). By contrast, MS analyzers coupled to gas chromatography (GC) or high-performance liquid chromatography (HPLC) offer a high sensitivity, becoming a highly feasible and informative technique that has demonstrated its potential in human metabolomic studies (*Castro-Puyana & Herrero, 2013*; *Xu et al., 2009*). Besides, both NMR- and MS-based metabolomics rely on wide-untargeted approaches, but MS also allows retrospective analysis of relevant metabolites by means of the full-spectra acquisition by quadrupole time-of-flight mass analyzer (QTOF). Taking in mind all these constraints and advantages, a major aim of this study was to demonstrate the validity of metabolomics based on ultra-high performance liquid chromatography (UHPLC) and high resolution MS (HRMS) to provide new insights on the nutritional and metabolic phenotyping of farmed fish. To this end, the present work was conceived as a MS approach to identify and, most importantly, validate robust biomarkers of malnutrition in short-term fasted fish, using gilthead sea bream (*Sparus aurata*) as a model of a highly cultured fish in all the Mediterranean basin.

MATERIALS & METHODS

Reagents and chemicals
HPLC-grade water was obtained from a Mili-Q water purification system (Millipore Ltd., Bedford, MA, USA). HPLC-grade methanol (MeOH), HPLC-supergradient acetonitrile (ACN), sodium hydroxide (>99%) and reagent grade ammonium acetate (NH_4Ac) were obtained from Scharlab (Barcelona, Spain). Leucine-enkephalin (mass-axis calibration), formic acid (mobile phase modifier) and analytical-grade standards methionine sulfoxide and trimethylamine N-oxide were purchased from Sigma-Aldrich (Saint Louis, MO, USA).

Animal care and sampling
Two-year-old gilthead sea bream of Atlantic origin (average initial weight: 380 g) were reared from early life stages in the indoor experimental facilities of the Institute of Aquaculture Torre de la Sal (IATS), following natural light and temperature conditions at our latitude (40°5′N, 0°10′E). The oxygen content of water was always higher than 85% saturation, unionized ammonia remained below toxic levels (<0.02 mg/l), and rearing density was maintained lower than 15 kg/m^3.

At mid-summer (July 2014), 30 fish were randomly allocated in two tanks (500 L). One group continued to be fed with a standard commercial diet (Biomar, EFICO Forte 824) to visual satiety one time per day, whereas the other group remained unfed for a 10-day period. At the end of this period, 10 fish from fasted and fed groups (following overnight fasting) were randomly sampled and anaesthetized with 100 mg/L of aminobenzoic acid ethyl ester (MS-222, Sigma-Aldrich) for blood and tissue sampling. Blood was taken from caudal vessels with vacutainer tubes with a clot activator. Liver and visceral adipose tissue were extracted and weighed. Blood samples were allowed to clot for 30 min at room temperature, and then centrifuged at 1,300 g for 10 min. The obtained samples were stored at −20 °C until analysis.

All procedures were approved by the IATS Ethics and Animal Welfare Committee according to national (Royal Decree RD53/2013) and EU legislation (2010/63/EU) on the handling of animals for experiments.

Sample processing

Serum samples were centrifuged at 12,500 g for 10 min. Supernatant (400 μL) was diluted with 1.2 mL of ACN followed by centrifugation (12,500 g for 10 min). Then, 750 μL of supernatant were stored for hydrophilic interaction liquid chromatography (HILIC), and another 750 μL aliquot was evaporated to dryness by MiVac Duo Concentrator (40 °C, 60 min) and dissolved with MeOH (75 μL) and Mili-Q Water (675 μL) for reversed phase (RP) analysis (details in Fig. S1). Quality control (QC) samples were prepared by pooling 50 μL of each sample extract. All samples were stored at −20 °C until injection.

UHPLC-HRMS

A Waters Acquity UPLC system (Waters, Milford, MA, USA) was coupled to a hybrid quadrupole-TOF mass spectrometer (Xevo G2 QTOF, Waters, Manchester, UK), using a Z-spray-ESI interface operating in positive and negative ionization mode. The UHPLC separation was performed using Acquity UPLC® BEH C18 1.7 μm particle size analytical column 100 × 2.1 mm (Waters) at 300 μL/min flow rate for RP analysis. An Acquity UPLC® HILIC 1.7 μm particle size analytical column 100 × 2.1 mm (Waters) at 300 μL/min flow rate was used for hydrophilic interaction phase separations.

Each serum sample was injected four times, depending on the procedure (RP and HILIC) and the ionization mode selected (ESI+ and ESI−). The RP separation was performed using H_2O with 0.01% formic acid (HCOOH) as weak mobile phase (A) and MeOH with 0.01% HCOOH as strong mobile phase (B). The percentage of B was changed from 10% at 0 min, to 90% at 14 min, 90% at 16 min and 10% at 16.01 min, with a total run time of 18 min for both ESI+ and ESI−. For HILIC separation, the weak mobile phase was a mix of $ACN:H_2O$ (95:5, v/v) with 0.01% HCOOH and 10 mM NH_4Ac (A), and the strong mobile phase was H_2O with 0.01% HCOOH and 10 mM NH_4Ac (B). The B percentage was changed as follows: 0 min, 2%; 1.5 min, 2%; 2.5 min, 15%; 6 min, 50%; 7.5 min, 75%; and finally at 7.51 min, 2%, with a total run time of 10 min, for both ESI+ and ESI−. Sample injection volume was 10 μL in all cases. Nitrogen was used as both the desolvation gas and the nebulizing gas. A capillary voltage of 0.7 kV and 1.5 kV for positive and negative ion modes,

respectively, and cone voltage of 25 V were used. MS data were acquired over a m/z range of 50–1,200. TOF-MS resolution was approximately 20,000 at full width half maximum at m/z 556.2771. Collision gas was argon 99.995% (Praxair, Valencia, Spain). The desolvation gas flow was set at 1,000 L/h, and the cone gas was set at 80 L/h. Desolvation gas temperature was set to 600 °C, source temperature to 130 °C and column temperature to 40 °C.

For MS^E experiments, two acquisition functions with different collision energies were created. The low energy (LE) function, with a fixed collision energy of 4 eV, and the high energy (HE) function, with a collision energy ramp ranging from 15 to 40 eV in order to obtain the (de)protonated ion from LE function and a wide range of fragment ions from the HE function. Both LE and HE functions used a scan time of 0.3 s with an inter-scan delay of 0.05 s. MS/MS experiments were carried out in the same conditions with different collision energies depending on the fragmentation observed for each compound. Calibrations were conducted from m/z 50 to 1,200 with a 1:1 mixture of 0.05 M NaOH:5% HCOOH diluted (1:25) with H_2O:ACN (20:80), at a flow rate of 10 μL/min. For automated accurate mass measurement, a leucine-enkephalin solution (0.5 μg/mL) in ACN:H_2O (50:50) at 0.1% HCOOH was pumped at 30 μL/min through the lock-spray needle and measured every 30 s, with a scan time of 0.3 s. The (de)protonated molecule of leucine-enkephalin, at m/z 556.2771 in positive mode and m/z 554.2615 in negative mode was used for recalibrating the mass axis during the injection and to ensure a robust accurate mass along time.

Data processing

The workflow of data processing is shown in Fig. 1. LC-MS spectral data were converted from proprietary (*.raw,* Waters Corp.) to generic *(.cdf,* NetCDF) format using Databridge application (within MassLynx v 4.1; Waters Corporation) and processed using XCMS R package (https://xcmsonline.scripps.edu/) (*Smith et al., 2006*). *Centwave* feature detection algorithm was employed for peak picking (peak width from 5 to 20 s, S/N ratio higher than 10 and mass tolerance of 15 ppm) followed by retention time alignment for the detected features. Peak area normalization (mean centering) was applied to each data set in order to minimize instrumental drifts with a final log2 transformation to the area to standardize the range of independent feature variance followed by pareto scaling. ANOVA analysis followed by Benjamini–Hochberg multiple testing correction was applied to the normalized peak areas of all metabolites to assess differences between fed and control groups.

Multivariate analysis of processed metabolomics data was performed by means of the EZ-Info software (Umetrics, Sweden). First, Principal Component Analysis (PCA) was employed to ensure the absence of outliers and the correct classification of QCs after normalization. Partial Least Squares—Discriminant analysis (PLS-DA) was then applied to maximize the separation of fed and fasted individuals (*Fonville et al., 2010*). Orthogonal PLS-DA (OPLS-DA) was also carried out (*Wiklund et al., 2008*) with a high threshold (P[corr] > 0.95) for highlighting the most robust biomarkers.

For elucidation, the MS/MS spectra of the most significant metabolites were compared with reference spectra databases (METLIN, http://metlin.scripps.edu; Human Metabolome DataBase, http://www.hmbd.ca; MassBank, http://www.massbank.eu). For unassigned metabolites, *in silico* fragmentation software (MetFrag, http://msbi.ipb-halle.de/MetFrag)
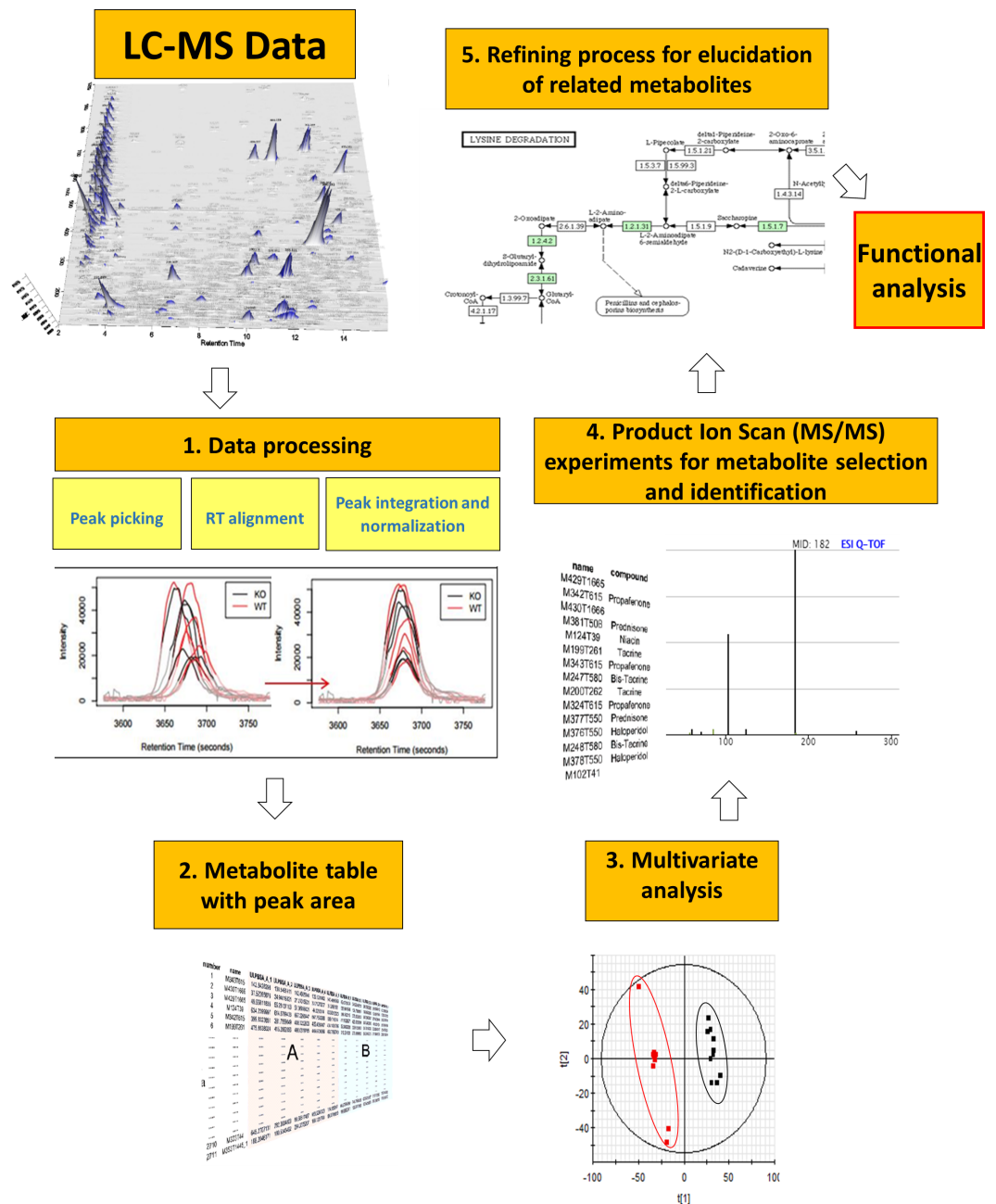
Figure 1 General metabolomics workflow from data acquisition by LC-MS to functional analysis.

was employed, with subsequent searches through Chemspider (http://www.chemspider.com) and PubChem (https://pubchem.ncbi.nlm.nih.gov) chemical databases. Injection of standards of methionine sulfoxide and trimethylamine N-oxide served to validate the elucidation workflow.

A retrospective analysis of data previously acquired in MS^E mode served for the refined search of additional relevant metabolites. It consisted in the search of the m/z ratio (parent ions) of the metabolites of interest in the LE function as well as product ions obtained from

Table 1 Biometry of fed (control) and fasted gilthead sea bream.

	Control	Fasted	*P*-value
Body weight (g)	426.5 ± 14.1	361.6 ± 10.7	0.002
Length (cm)	24.5 ± 0.3	24.0 ± 0.2	0.196
Condition factor	2.91 ± 0.06	2.63 ± 0.07	0.008
Liver weight (g)	5.63 ± 0.33	3.24 ± 0.16	4E−6
Mesenteric fat (g)	7.20 ± 1.08	6.01 ± 0.89	0.408
HSI (%)[a]	1.32 ± 0.05	0.90 ± 0.03	1E−6
MSI (%)[b]	1.90 ± 0.21	1.64 ± 0.23	0.394

Notes.
[a] Hepatosomatic index = (100 × liver weight)/body weight.
[b] Mesenteric fat index = (100 × mesenteric fat)/body weight.

MS/MS spectrum online databases (METLIN and Human Metabolome DataBase) in the HE function. Integrated areas of each candidate (parent ion) were compared in samples from fed and fasted groups.

RESULTS & DISCUSSION

Biometric data

At the end of the experimental period, body weight of fed fish was 15% higher than in fasted fish. This fasting protocol reduced the body fat depots, decreasing significantly ($P < 0.001$) the hepatosomatic index (100 × liver weight/body weight) from 1.3 to 0.9. The similar trend was found for mesenteric fat, although the decrease of mesenteric fat index (100 × mesenteric fat weight/body weight) from 1.9 to 1.6 was not statistically significant (Table 1). The magnitude of these changes was on the range of expected values for one- and two-year-old fish under similar experimental conditions (*Benedito-Palos, Ballester-Lozano & Pérez-Sánchez, 2014*; *Bermejo-Nogales, Calduch-Giner & Pérez-Sánchez, 2015*).

Untargeted metabolomics fingerprinting

Despite of the great potential of GC for chromatographic separation, the nature of serum samples, with medium-high polar compounds in a water-based fluid, pointed out to LC as a more convenient separation technique. UHPLC with sub-2 μm particle size was applied due to its high reproducibility and high separation performance in short-run time analyses. The use of different chromatographic techniques is a key issue to achieve a maximum of detected features when dealing with complex matrices like blood. In our case, serum samples were analyzed with two ionization modes and two different chromatographic columns: RP for a better separation of non-polar compounds, and HILIC to best separate the most polar compounds. In the RP analysis, 6,961 and 3,047 features were detected in both positive and negative ionization modes, while 4,820 and 1,015 features were labeled by XCMS using HILIC separation. This high total number of detected features (m/z values) highlights the huge detection power and sensitivity of HRMS and makes feasible a wide-view of sample composition to discriminate the most robust markers of nutritional conditions. Many features were only observed under a single ionization mode and chromatography type, reinforcing the importance of employing different chromatographic columns. As
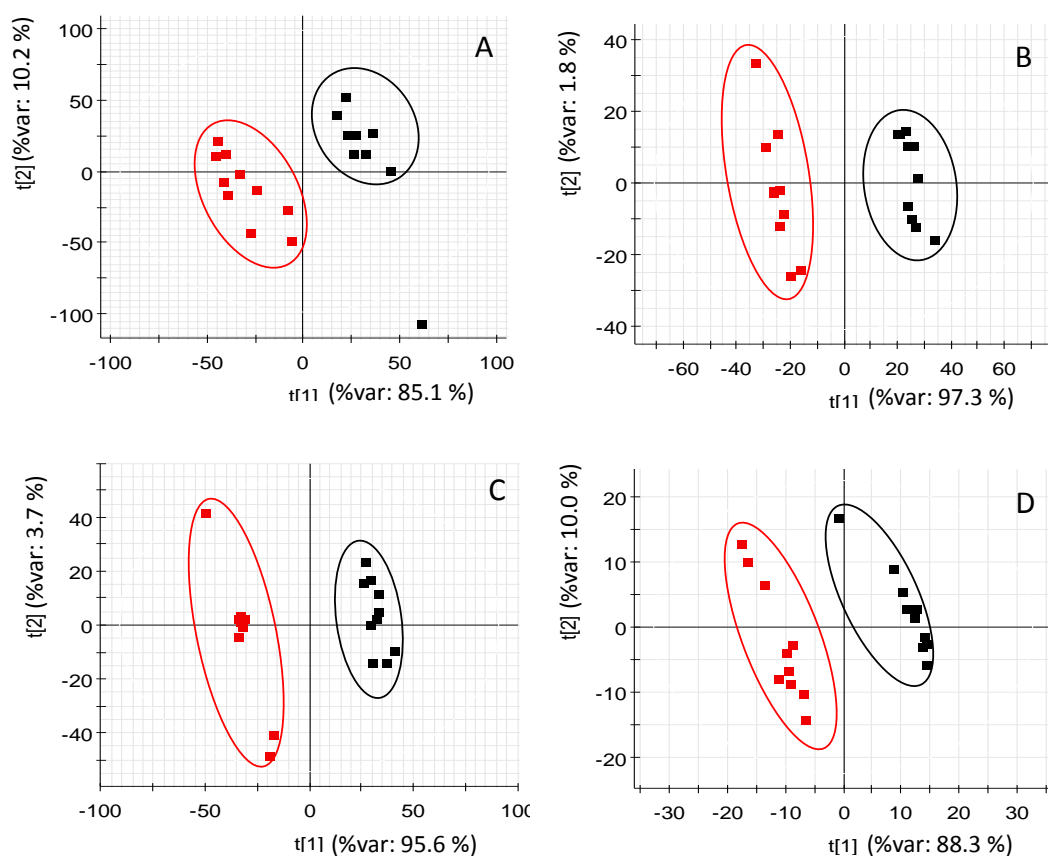
Figure 2 **PLS-DA score plots of acquired data of fasted (red) and control (black) fish.** X-axis corresponds to first component and Y-axis to second component (A) RP at positive ionization mode (B) RP at negative ionization mode (C) HILIC at positive ionization mode (D) HILIC in negative ionization mode.

an example, a single peak was detected by HILIC for the significant feature elucidated as LysoPC(20:5) while RP chromatography was able to separate ω-3 and ω-6 isomers (Fig. S2).

PLS-DA (of RP and HILIC in both positive and negative ionization modes) clearly discriminated the fasted individuals from those of the fed group (Fig. 2). Both groups were separated along the first component of the analysis, which explained 85–97% of the total variance. Individuals of the same group were distributed along the second PLS-DA component (2–10% of total variance). In the case of OPLS-DA, around 850 features from all four datasets were highlighted as discriminatory between fed and fasted fish with a $P[\text{corr}] > 0.95$ and a corrected P-value < 0.05 (see Fig. S3). Among them, up to 45 different compounds were elucidated as amino acids (4), oligopeptides (8), urea cycle-related metabolites (2), acylcarnitines (5), glutathione-related compounds (5), fatty acids (5), 3-hydroxyisovaleric acid, 3-methoxy-4-hydroxy-phenylglycol (MOPEG) sulphate and phospholipids (14), including phosphatidylcholines (PC) and lysoPC (Table 2).

Phospholipids were characterized by the presence of both the protonated molecule and sodium adduct in the positive LE spectra and their acetate adducts in negative LE spectra. As an example, Fig. S4 shows the m/z 542.3248 (+0.1 mDa mass error) which corresponds to the protonated molecule, and m/z 564.3074 (+1.2 mDa mass error) corresponds to the

Table 2 Compound list obtained from untargeted approach and refining process.

	Compound name	Biological process[a]	Chromatography/ ionization mode[b]	Formula	De/protonated molecule m/z (error mDa)	RT (min)	Change (%) from CTRL[c]	Corrected P-value[d]
1	Octanoyl-L-carnitine	1, 2	RP/+	$C_{15}H_{29}NO_4$	288.2158 (−1.8)	10.38	373%	3.1E−06
2	Decanoyl-L-carnitine	1, 2	RP/+	$C_{17}H_{33}NO_4$	316.2478 (−1.0)	12.58	492%	4.53E−07
3	Hexadecenedioic acid mono-L-carnitine ester	1, 2	RP/+	$C_{23}H_{43}NO_6$	430.3157 (−1.2)	13.28	373%	1.15E−06
4	Tetradecadien-L-carnitine	1, 2	RP/+	$C_{21}H_{37}NO_4$	368.2784 (−1.7)	8.90	373%	1.25E−05
5	Tetradecenoyl-L-carnitine	1, 2	RP/+	$C_{21}H_{39}NO_4$	370.2947 (−1.0)	14.88	373%	9.98E−06
6	L-ornithine	3, 4	RP/+	$C_5H_{12}N_2O_2$	133.0972 (−0.5)	5.29	1213%	1.26E−10
7	Citrulline[e]	3, 4	HI/+	$C_6H_{13}N_3O_3$	176.1029 (−0.6)	5.30	140%	5.02E−03
8	Argininosuccinate[e]	3, 4	HI/−	$C_{10}H_{18}N_4O_6$	289.1145 (−0.3)	1.31	248%	2.07E−02
9	Norvaline	3, 4	RP/−	$C_5H_{11}NO_2$	116.0711 (−0.1)	2.51	29%	5.54E−08
10	L- Arginine[e]	3, 4	HI/+	$C_6H_{14}N_4O_2$	175.1194 (−0.1)	6.14	128%	3.37E−02
11	N-(2-cyanoethyl)glycine	3	HI/+	$C_5H_8N_2O_2$	129.0673 (+0.9)	5.25	246%	6.05E−09
12	Isoleucine	3	RP/−	$C_6H_{13}NO_2$	130.0880 (+1.4)	1.61	230%	1.15E−06
13	Glutamine	3	HI/+	$C_5H_{10}N_2O_3$	147.0766 (−0.4)	5.15	214%	1.80E−05
14	Glu-Phe	3	RP/+	$C_{14}H_{18}N_2O_5$	295.1278 (−1.6)	4.61	23%	9.11E−07
15	His-Phe	3	RP/+	$C_{15}H_{18}N_4O_3$	303.1447 (−1.0)	2.08	50%	6.53E−05
16	LTYV	3	RP/−	$C_{24}H_{38}N_4O_7$	493.2652 (−1.0)	5.80	23%	9.98E−06
17	LLGGPS	3	RP/+	$C_{24}H_{42}N_6O_8$	543.3148 (+0.6)	6.48	214%	2.53E−05
18	QLWD	3	RP/+	$C_{26}H_{36}N_6O_8$	561.2688 (+1.5)	8.08	373%	4.58E−04
19	YLWV	3	RP/+	$C_{24}H_{38}N_4O_7$	495.2807 (−1.2)	8.10	283%	2.77E−04
20	SVLGPA	3	RP/+	$C_{24}H_{42}N_6O_8$	543.3141 (−0.1)	14.75	746%	2.87E−07
21	N(2-Furoyl)glycyl-leucine	3	RP/−	$C_{13}H_{20}N_2O_5$	283.1301 (+0.7)	5.15	303%	3.44E−09
22	MOPEG sulphate	5	RP/−	$C_9H_{12}O_7S$	263.0223 (−0.2)	2.01	325%	9.70E−07
23	Noradrenaline[e]	5	HI/+	$C_8H_{11}NO_3$	170.0806 (−1.1)	3.02	141%	9.34E−03
24	DOPEGAL[e]	5	HI/+	$C_8H_8O_4$	169.0501 (0.0)	3.11	229%	3.94E−07
25	DOPEG[e]	5	HI/+	$C_8H_{10}O_4$	171.0649 (−0.8)	2.55	108%	1.94E−01
26	ϒ-Glu-Leu	6	HI/+	$C_{11}H_{20}N_2O_5$	261.1432 (−1.8)	3.37	246%	3.13E−06
27	ϒ-Glu-Val	6	RP/+	$C_{10}H_{18}N_2O_5$	247.1285 (−0.9)	2.15	246%	1.05E−08
28	ϒ-Glu-Ile	6	HI/+	$C_{11}H_{20}N_2O_5$	261.1446 (−0.4)	3.12	696%	1.48E−08
29	Pyroglutamic acid	6	HI/+	$C_5H_7NO_3$	130.0521 (−1.7)	5.15	303%	4.26E−06
30	Glutathione[e]	6	HI/−	$C_{10}H_{17}N_3O_6S$	306.0760 (0.0)	1.37	66%	3.03E−02
31	γ-Glu-Cys[e]	6	HI/+	$C_8H_{14}N_2O_5S$	251.0701 (−0.1)	4.92	63%	4.22E−01
32	Methionine sulfoxide	6	HI/+	$C_5H_{11}NO_3S$	166.0511 (−0.2)	4.96	41%	2.08E−04

Table 2 (*continued*)

	Compound name	Biological process[a]	Chromatography/ ionization mode[b]	Formula	De/protonated molecule m/z (error mDa)	RT (min)	Change (%) from CTRL[c]	Corrected P-value[d]
33	FFA (C18:3)	1, 2	RP/−	$C_{18}H_{30}O_2$	277.2172 (−0.4)	15.41	246%	2.08E–04
34	9-hydroxy-octadecanoic acid	1, 2	RP/−	$C_{18}H_{36}O_3$	299.2598 (+1.3)	14.98	528%	2.23E–07
35	Linoleic acid	1, 2	RP/−	$C_{20}H_{34}O_2$	305.2500 (+1.9)	16.31	19%	3.43E–06
36	Eicosapentaenoic acid	1, 2	RP/−	$C_{20}H_{30}O_2$	301.2152 (−1.6)	15.10	33%	2.01E–03
37	Acetohexadecyloxy propylaminoethyl phosphate	1, 7	RP/+	$C_{23}H_{48}NO_7P$	482.3250 (+0.3)	14.93	35%	2.53E–06
38	LysoPC(14:0)	1, 7	RP/+	$C_{22}H_{46}NO_7P$	468.3083 (−0.7)	15.41	25%	9.29E–05
39	LysoPC(16:1)	1, 7	RP/+	$C_{24}H_{48}NO_7P$	494.3244 (−0.3)	14.91	44%	1.71E–04
40	LysoPC(18:4)	1, 7	RP/+	$C_{26}H_{46}NO_7P$	516.3079 (−1.1)	14.36	11%	1.40E–08
41	LysoPC(18:3)	1, 7	RP/+	$C_{26}H_{48}NO_7P$	518.3247 (0.0)	14.38	4%	1.93E–11
42	LysoPC(20:5)	1, 7	RP/+	$C_{28}H_{48}NO_7P$	542.3248 (+0.1)	14.58	13%	1.37E–08
43	LysoPC(18:1)	1, 7	RP/+	$C_{26}H_{52}NO_7P$	522.3560 (0.0)	15.00	16%	8.10E–08
44	LysoPC(21:5)	1, 7	RP/+	$C_{29}H_{50}NO_7P$	556.3408 (+0.5)	14.88	31%	9.98E–06
45	LysoPC(20:4)	1, 7	RP/+	$C_{28}H_{50}NO_7P$	544.3411 (+0.8)	14.06	20%	7.01E–06
46	LysoPC (Tetradecylthioacetic acid)	1, 7	RP/+	$C_{24}H_{48}NO_7PS$	526.2951 (−1.6)	15.13	1%	1.62E–09
47	PC(22:5/20:5)	1, 7	HI/+	$C_{50}H_{80}NO_8P$	854.5689 (−1.1)	4.11	27%	3.01E–08
48	PC(20:5/18:1)	1, 7	HI/+	$C_{46}H_{78}NO_8P$	804.5435 (−0.8)	6.78	200%	1.95E–02
49	PC(20:4/18:1)	1, 7	HI/+	$C_{46}H_{82}NO_8P$	808.5843 (−1.3)	5.73	214%	4.69E–02
50	PC(18:1/16:0)	1, 7	HI/+	$C_{42}H_{82}NO_8P$	760.5847 (−0.9)	4.06	303%	1.79E–05
51	TMAO	1, 7	HI/+	C_3H_9NO	76.0760 (−0.2)	5.85	41%	7.68E–05
52	Glycerophos phocholine	1, 7	HI/+	$C_8H_{20}NO_6P$	258.1106 (0.0)	5.73	12%	5.69E–05
53	Hydroxyisovaleric acid	8	RP/−	$C_5H_{10}O_3$	117.0553 (+0.1)	2.85	373%	2.41E–09
54	Biotin[e]	8	RP/+	$C_{10}H_{16}N_2O_3S$	245.0959 (−0.1)	5.40	80%	2.46E–01

Notes.

[a] 1, Lipid metabolism; 2, Fatty acid metabolism; 3, Protein metabolism; 4, Amino catabolism/urea-cycle; 5, Stress response/catecholamine metabolism; 6, Oxidative stress/glutathione metabolism; 7, Phospholipid metabolism; 8, Vitamin metabolism.

[b] Chromatography and ionization modes in which the signal area was higher for the highlighted compound.

[c] Variation of area between fed and fasted fish. Variation > 100% means higher area in fasted fish, and <100% means lower are in fasted fish.

[d] ANOVA followed by Benjamini–Hochberg multiple testing correction.

[e] Compounds obtained in refining process.

sodium adduct in RP+. MS/MS experiments were also carried out obtaining m/z 184.0735 (-0.4 mDa) (main product ions at 30 eV) in positive ionization mode. These m/z ions were annotated as phosphocholine in agreement with fragmentation pathways of lysoPC (*Xu et al., 2009*; *González-Domínguez, García-Barrera & Gómez-Ariza, 2014*).

Carnitine-related compounds were also elucidated after MS/MS experiments by the presence of m/z 144.1051 ($C_7H_{13}NO_2^+$, $+2.6$ mDa), 85.0303 ($C_4H_5O_2^+$, $+1.3$ mDa) and 60.0814 ($C_3H_{10}N^+$, -0.3 mDa) as characteristic product ions of these compounds (*Möder et al., 1997*; *Luci, Hirche & Eder, 2008*) also observed in METLIN spectra for some of these compounds (Fig. S5).

Tandem mass spectrometry also provides relevant information for isomers differentiation. For example, γ-Glu-Ile and γ-Glu-Leu presented the same molecular formula and close retention times (Fig. S6). MS/MS experiments revealed very similar spectra at 10 and 20 eV with the exception of the m/z 142.0499 which only appeared for the peak at 3.37 min. After comparing both spectra with METLIN, only γ-Glu-Leu spectrum showed this m/z ion at 20 eV. The formation of $C_4H_8^+$ have been observed and described in the literature much higher in isoleucine than in leucine (*Squire, Beranová & Wesdemiotis, 1995*), so in leucine spectra the neutral loss of C_4H_8 can be observed while it does not appears in isoleucine spectra. This strategy was followed for the rest of elucidated compounds.

Functional analysis of elucidated compounds

Biological significance of the concurrent up- or down-regulation of most of the elucidated metabolites during fasting clearly stated that food deprivation increased mobilization of body energy stores and improved the oxidative capacity of metabolic fuels, which paralleled the onset of specific changes in the cell redox-balance. In this regard, the increased mobilization of body fat stores in fasted individuals, exemplified by the loss of liver and adipose tissue mass, was linked to the consistent increase of circulating levels of five sub-products of L-carnitine (compounds 1–5 in Table 2), a carrier of fatty acids across the inner mitochondrial membrane for their subsequent beta-oxidation (*Luci, Hirche & Eder, 2008*; *Ball, Urschel & Pencharz, 2007*). At the molecular level, this was early substantiated in similar experimental conditions by a marked up-regulated expression of the two carnitine palmitoyltransferase variants (CPT1A, CPT1B) of the skeletal muscle of gilthead sea bream (*Benedito-Palos, Ballester-Lozano & Pérez-Sánchez, 2014*), which was encompassed by the increased expression of a high representation (25 enzyme subunits) of regulatory and assembly factors of the five enzyme complex units (Complex I–V) of the mitochondrial respiratory chain (*Bermejo-Nogales, Calduch-Giner & Pérez-Sánchez, 2015*). Microarray gene expression profiling of either glycolytic or aerobic muscle tissues of fish fed to maintenance ration also indicates that nutrient scarcity is by itself a major factor driving switches in muscle protein turnover and mitochondrial activity (*Calduch-Giner et al., 2014*). In the present study, this was reinforced by the consistent fasting increase of serum concentrations of urea cycle-related compounds (citrulline, ornithine, argininosuccinate and arginine). Of note, the activity of urea cycle enzymes is typically higher in carnivorous fish than in herbivorous and omnivorous fish species (*Chiu, Austic & Rumsey, 1986*), and our results highlighted

that acyl-carnitine and urea cycle metabolites are specially sensitive to fasting-mediated changes in fatty acid and amino acid catabolism during negative energy balance.

Catecholamines are mobilized into fish circulation during a variety of stressful situations which require modulation of cardiorespiratory function or mobilization of energy reserves. The magnitude of change is dependent on the species and the type and intensity of stress imposed, although a wide range of stressors including hypoxia, hypercapnia, exhaustive and violent exercise, air exposure or anemia are considered strong activators of the hypothalamic-pituitary-interrenal (HPI) axis in fish (*Reid, Bernier & Perry, 1998*). This also applies to short-term fasting (*De Pedro et al., 2003*), and the observed increase of MOPEG sulphate, a metabolite of norepinephrine degradation, can be viewed as part of the adaptive response of the HPI axis to cope with fasting hypoglycemia through the activation of lipolysis and gluconeogenesis. This notion was supported by the increased levels of nora-drenaline, and other catecholamine metabolites 3,4-dihydroxymandelaldehyde and 3,4-dihydroxyphenylethyleneglycol (DOPEGAL and DOPEG), detected in the refined search step of analysis.

The primary enzymatic antioxidant defense system of living organisms is the glutathione (GSH) redox system that reduces hydrogen peroxide and lipid hydroperoxides at the expense of oxidizing GSH to its disulfide form (GSSG). Once oxidized, GSH can be reduced back by glutathione reductase, using NADPH as an electron donor, and previous studies in gilthead seam bream indicate that either absolute GSH levels or the GSH/GSSG ratio are regulated by dietary oils, increasing the total plasma antioxidant capacity with the increased unsaturation index of dietary oils of marine origin (*Saera-Vila et al., 2005*). Likewise, total plasma antioxidant capacity is increased in hypoxic fish with a switch from oxidative phosphorylation (OXPHOS) to anaerobic glycolysis (*Bermejo-Nogales, Calduch-Giner & Pérez-Sánchez, 2014*), which results in reduced mitochondria oxygen consumption and enhanced NADH production from glycolysis (*Frezza et al., 2011*). Importantly, extension of life span is related in mammals and birds to low antioxidant levels and low rates of generation of reactive oxygen species (ROS) (*Lykkesfeldt & Svendsen, 2007*; *Pamplona et al., 2008*). Experimental evidence in rats also indicates that intermittent fasting affects redox balance in a tissue selective manner (*Chausse et al., 2015*), and our fish metabolomic study highlighted that the depletion of serum GSH during short-term fasting was closely related to changes in the Meister's γ-glutamyl cycle with a key role in the recovery and delivery of cysteine in the body (*Griffith, Bridges & Meister, 1978*). This was supported by high circulating concentrations of ϒ-Glu-(Leu/Val/Ile) and pyroglutamic acid in the serum of fasted gilthead sea bream, whereas both GSH and ϒ-Glu-Cys were depleted ([Fig. 3]). This represents a complex trade-off with a reduced risk of oxidative stress, also highlighted by the decreased concentration of methionine sulfoxide, an oxidized form of methionine that is highly correlated with the risk of oxidative stress (*Weissbach et al., 2002*). In parallel, other short oligopeptides were either increased or decreased in the serum of fasted fish. It remains to be established if they have a physiological significance or are subproducts of protein hydrolysis.

The fatty acid composition of triacylglycerols (TAG) usually clears a close resemblance to dietary lipids (*Benedito-Palos et al., 2010*), whereas that of phospholipids is highly regulated
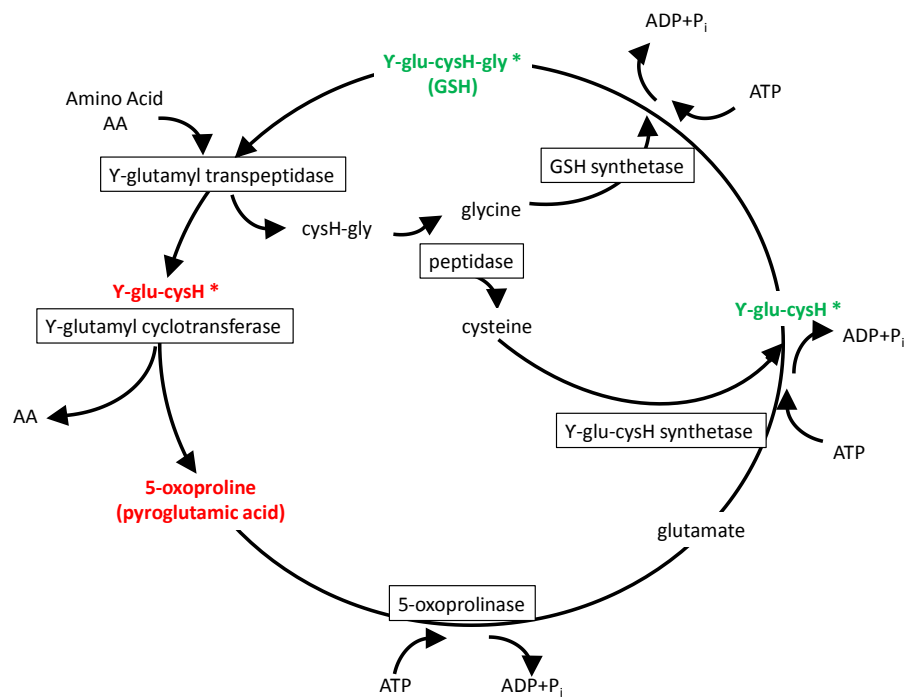
Figure 3 **Meister's cycle.** In red, elucidated metabolites up-regulated with fasting; in green, down-regulated with fasting. Asterisks mark elucidated metabolites by means of the refining step.

and influenced in fish by environmental factors, including temperature and osmolarity (*Los & Murata, 2004*; *Ibarz et al., 2005*). The specific effects of ration size have been addressed in gilthead sea bream, and maintenance ratio significantly increased the retention of arachidonic acid (ARA) and docosahexanoic acid (DHA) in muscle phospholipids, whereas the fatty acid composition of storage lipids remained almost unchanged (*Benedito-Palos et al., 2013*). This lean muscle phenotype was linked in the present study to low plasma levels of linoleic acid and eicosapentaenoic acid, the precursors of ARA and DHA, respectively. At the same time, fasting induced an overall decrease of circulating lysoPC and glycerophosphocholine, whereas the effect on phosphatydylcholines was more selective depending of the composition of fatty acids. In any case, phospholipid metabolism is becoming highly regulated by feed intake at either blood or tissue level. Thus, phospholipids of skeletal muscle would act as a reservoir of long chain poly-unsaturated fatty acids with an enhanced expression of lipoprotein lipase-like, a TAG lipase isoform exclusive of fish linage which is highly expressed in muscle tissues and specifically up-regulated by feed restriction (*Benedito-Palos et al., 2013*; *Rimoldi et al., 2015*). This in turn would mediate, at least in part, the changes in the blood composition of phospholipid-related metabolites. This is extensive to trimethylamine N-oxide (TMAO), and high TMAO and choline concentrations are associated in humans with diabetes and advanced cardio-metabolic risk profile (*Obeid et al., 2016*). In agreement with this, the opposite pattern was found herein in fish under a negative energy balance, which reinforces the close metabolic association between interrelated pathways of phospholipid and oxidative metabolism. Recent metabolomics studies have

	METABOLITES	BIOLOGICAL PROCESS	SIGNIFICANCE
🔴	L-carnitines	Fatty acid oxidation	Enhanced mobilization of lipid depots & muscle protein breakdown
🔴 🟢	Urea cycle metabolites	Amino acid catabolism	
🔴	Catecholamines	Lipolysis/Gluconeogenesis	Regulation of glucose homeostasis
🔴 🟢	Glutathione-related metabolites	Meister's cycle	Recovery and delivery of cysteine in the body
🔴 🟢	Fatty acids, Phosphatidylcholines and LysoPhosphatidylcholines	Fatty acid/Phospholipid metabolism	Increased retention of long chain poly-unsaturated fatty acids
🔴 🟢	3-Hydroxyisovaleric acid and biotin	Biotin metabolism	Signs of vitamin deficiency

Figure 4 Corollary with the metabolic significance of highlighted metabolites. Red and green circles signals the degree of up- and down-regulation of metabolites, respectively, with fasting.

highlighted a concurrent depletion of reduced GSH and glycerophosphocholine in the gills of another fish species, the golden grey mullet (*Liza aurata*), as a response to mercury toxicity (*Cappello et al., 2016a*; *Cappello et al., 2016b*). This finding also reinforces the view that the response to different challenges such as malnutrition or pollutants toxicity and susceptibility (*Kokushi et al., 2016*; *Wang et al., 2016*) can be assessed by the analysis of common responsive metabolites, opening the possibility for future screening of the fish general welfare status through selected biomarkers.

Lastly, major changes in vitamin status are related in our experimental model to biotin metabolism. In humans, the impairment of renal reclamation of biotin results in an elevated urine concentration of 3-hydroxyisovaleric acid (*Mock et al., 1997*). Accordingly, we found that the fasting increase of this metabolite was concurrent with a low biotin availability (highlighted by refining analysis), which reinforces the role of 3-hydroxyisovaleric acid as a biomarker of B7 vitamin deficiency in a wide range of vertebrate species, including fish.

CONCLUSIONS

This metabolomics study has been performed to help fish physiologists and nutritionists to identify highly sensitive and robust biomarkers of malnutrition from a large list of affected compounds (about 850 ions) (see Fig. 4 as a corollary). The MS^E acquisition mode of the involved QTOF allowed to simultaneously recording both low and high collision energy mass spectra. In this sense, as full scan data is acquired, the possibility of refining steps after elucidation gives HRMS a strong advantage compared to NMR. Further studies are underway to determine the potential of this powerful methodological approach, alone or in combination with other omics approaches, for the discovery and validation of new

biomarkers of nutritional status in a wide-range of physiological conditions arising with the advent of new fish feed formulations.

ACKNOWLEDGEMENTS

This work has been developed in the framework of the Research Unit of Marine Ecotoxicology (IATS (CSIC)-IUPA (UJI)).

Funding

This work was supported by the Spanish MINECO (MI2-Fish, AGL2013-48560) and Plà de promoció de la investigació de la Universitat Jaume I (P1●1B2015-59) and the Generalitat Valenciana as research group of excellence (PROMETEO II/2014/023, PROMETEO II/2014/085, Collaborative Research on Environment and Food-Safety, ISIC/2012/016). The funders had no role in study design, data collection and analysis, decision to publish, or preparation of the manuscript.

Grant Disclosures

The following grant information was disclosed by the authors:
Spanish MINECO: MI2-Fish, AGL2013-48560.
Plà de promoció de la investigació de la Universitat Jaume I: P1●1B2015-59.
Generalitat Valenciana: PROMETEO II/2014/023, PROMETEO II/2014/085, ISIC/2012/016.

Competing Interests

The authors declare there are no competing interests.

Author Contributions

- Ruben Gil-Solsona, Jaime Nácher-Mestre and Josep Alvar Calduch-Giner performed the experiments, analyzed the data, contributed reagents/materials/analysis tools, wrote the paper, prepared figures and/or tables, reviewed drafts of the paper.
- Leticia Lacalle-Bergeron performed the experiments, analyzed the data, contributed reagents/materials/analysis tools, wrote the paper, reviewed drafts of the paper.
- Juan Vicente Sancho conceived and designed the experiments, analyzed the data, contributed reagents/materials/analysis tools, wrote the paper, prepared figures and/or tables, reviewed drafts of the paper.
- Félix Hernández conceived and designed the experiments, analyzed the data, contributed reagents/materials/analysis tools, wrote the paper, reviewed drafts of the paper.
- Jaume Pérez-Sánchez conceived and designed the experiments, performed the experiments, analyzed the data, contributed reagents/materials/analysis tools, wrote the paper, prepared figures and/or tables, reviewed drafts of the paper.
Animal Ethics

The following information was supplied relating to ethical approvals (i.e., approving body and any reference numbers):

All procedures were approved by the IATS Ethics and Animal Welfare Committee according to national (Royal Decree RD53/2013) and EU legislation (2010/63/EU) on the handling of animals for experiments.

Data Availability

The raw data has been supplied as Data S1.

Supplemental Information

Supplemental information for this article can be found online at http://dx.doi.org/10.7717/peerj.2920#supplemental-information.

REFERENCES

Asakura T, Sakata K, Yoshida S, Date Y, Kikuchi J. 2014. Noninvasive analysis of metabolic changes following nutrient input into diverse fish species, as investigated by metabolic and microbial profiling approaches. *PeerJ* **2**:e550 DOI 10.7717/peerj.550.

Ball RO, Urschel KL, Pencharz PB. 2007. Nutritional consequences of interspecies differences in arginine and lysine metabolism. *Journal of Nutrition* **137**:1626S–1641S.

Benedito-Palos L, Ballester-Lozano G, Pérez-Sánchez J. 2014. Wide-gene expression analysis of lipid-relevant genes in nutritionally challenged gilthead sea bream (*Sparus aurata*). *Gene* **547**:34–42 DOI 10.1016/j.gene.2014.05.073.

Benedito-Palos L, Ballester-Lozano GF, Simó P, Karalazos V, Ortiz Á, Calduch-Giner J, Pérez-Sánchez J. 2016. Lasting effects of butyrate and low FM/FO diets on growth performance, blood haematology/biochemistry and molecular growth-related markers in gilthead sea bream (*Sparus aurata*). *Aquaculture* **454**:8–18 DOI 10.1016/j.aquaculture.2015.12.008.

Benedito-Palos L, Calduch-Giner JA, Ballester-Lozano GF, Pérez-Sánchez J. 2013. Effect of ration size on fillet fatty acid composition, phospholipid allostasis and mRNA expression patterns of lipid regulatory genes in gilthead sea bream (*Sparus aurata*). *British Journal of Nutrition* **109**:1175–1187 DOI 10.1017/S000711451200311X.

Benedito-Palos L, Navarro JC, Kaushik S, Pérez-Sánchez J. 2010. Tissue-specific robustness of fatty acid signatures in cultured gilthead sea bream (*Sparus aurata* L.) fed practical diets with a combined high replacement of fish meal and fish oil. *Journal of Animal Science* **88**:1759–1770 DOI 10.2527/jas.2009-2564.

Bermejo-Nogales A, Calduch-Giner JA, Pérez-Sánchez J. 2014. Tissue-specific gene expression and functional regulation of uncoupling protein 2 (UCP2) by hypoxia and nutrient availability in gilthead sea bream (*Sparus aurata*): implications on the physiological significance of UCP1-3 variants. *Fish Physiology and Biochemistry* **40**:751–762 DOI 10.1007/s10695-013-9882-7.

Bermejo-Nogales A, Calduch-Giner JA, Pérez-Sánchez J. 2015. Unraveling the molecular signatures of oxidative phosphorylation to cope with the nutritionally changing metabolic capabilities of liver and muscle tissues in farmed fish. *PLOS ONE* **10**:e0122889 DOI 10.1371/journal.pone.0122889.

Calduch-Giner JA, Echasseriau Y, Crespo D, Baron D, Planas JV, Prunet P, Pérez-Sánchez J. 2014. Transcriptional assessment by microarray analysis and large-scale meta-analysis of the metabolic capacity of cardiac and skeletal muscle tissues to cope with reduced nutrient availability in gilthead sea bream (*Sparus aurata* L.). *Marine Biotechnology* **16**:423–435 DOI 10.1007/s10126-014-9562-3.

Cappello T, Brandão F, Guilherme S, Santos MA, Maisano M, Mauceri A, Canário J, Pacheco M, Pereira P. 2016a. Insights into the mechanisms underlying mercury-induced oxidative stree in gills of wild fish (*Liza aurata*) combining ^{1}H NMR metabolomics and conventional biochemical assays. *Science of the Total Environment* **548–549**:13–24 DOI 10.1016/j.scitotenv.2016.01.008.

Cappello T, Pereira P, Maisano M, Mauceri A, Pacheco M, Fasulo S. 2016b. Advances in understanding the mechanisms of mercure toxicity in wild golden grey mullet (*Liza aurata*) by ^{1}H NMR-based metabolomics. *Environmental Pollution* **219**:139–148 DOI 10.1016/j.envpol.2016.10.033.

Castro-Puyana M, Herrero M. 2013. Metabolomics approaches based on mass spectrometry for food safety, quality and traceability. *Trends in Analytical Chemistry* **52**:74–87 DOI 10.1016/j.trac.2013.05.016.

Chausse B, Vieira-Lara MA, Sanchez AB, Medeiros MHG, Kowaltowski AJ. 2015. Intermittent fasting results in tissue-specific changes in bioenergetics and redox state. *PLOS ONE* **10**:e0120413 DOI 10.1371/journal.pone.0120413.

Chiu YN, Austic RE, Rumsey GL. 1986. Urea cycle activity and arginine formation in rainbow trout (*Salmo gairdneri*). *Journal of Nutrition* **116**:1640–1650.

De Pedro N, Delgado MJ, Gancedo B, Alonso-Bedate M. 2003. Changes in glucose, glycogen, thyroid activity and hypothalamic catecholamines in tench by starvation and refeeding. *Journal of Comparative Physiology B* **173**:475–481 DOI 10.1007/s00360-003-0355-7.

Emwas A-HM. 2015. The strengths and weaknesses of NMR spectroscopy and mass spectrometry with particular focus on metabolomics research. *Methods in Molecular Biology* **1277**:161–193 DOI 10.1007/978-1-4939-2377-9_13.

Fonville JM, Richards SE, Barton RH, Boulange CL, Ebbels TMD, Nicholson JK, Holmes E, Dumas ME. 2010. The evolution of partial least squares models and related chemometric approaches in metabonomics and metabolic phenotyping. *Journal of Chemometrics* **24**:636–649 DOI 10.1002/cem.1359.

Frezza C, Zheng L, Tennant DA, Papkovsky DB, Hedley BA, Kalna G, Watson DG, Gottlieb E. 2011. Metabolic profiling of hypoxic cells revealed a catabolic signature required for cell survival. *PLOS ONE* **6**:e24411 DOI 10.1371/journal.pone.0024411.

González-Domínguez R, García-Barrera T, Gómez-Ariza JL. 2014. Combination of metabolomic and phospholipid-profiling approaches for the study of Alzheimer's disease. *Journal of Proteomics* **104**:37–47 DOI 10.1016/j.jprot.2014.01.014.

Griffith OW, Bridges RJ, Meister A. 1978. Evidence that the gamma-glutamyl cycle functions *in vivo* using intracellular glutathione: effects of amino acids and selective inhibition of enzymes. *Proceedings of the National Academy of Sciences of the United States of America* **75**:5405–5408 DOI 10.1073/pnas.75.11.5405.

Ibarz A, Blasco J, Beltrán M, Gallardo MA, Sánchez J, Sala R, Fernández-Borràs J. 2005. Cold-induced alterations on proximate composition and fatty acid profiles of several tissues in gilthead sea bream (*Sparus aurata*). *Aquaculture* **249**:477–486 DOI 10.1016/j.aquaculture.2005.02.056.

Jégou M, Gondret F, Lalande-Martin J, Tea I, Baéza E, Louveau I. 2016. NMR-based metabolomics highlights differences in plasma metabolites in pigs exhibiting diet-induced differences in adiposity. *European Journal of Nutrition* **55**:1189–1199 DOI 10.1007/s00394-015-0932-z.

Karalazos V, Bendiksen EÅ, Dick JR, Bell JG. 2007. Effects of dietary protein, and fat level and rapeseed oil on growth and tissue fatty acid composition and metabolism in Atlantic salmon (*Salmo salar* L.) reared at low water temperatures. *Aquaculture Nutrition* **13**:256–265 DOI 10.1111/j.1365-2095.2007.00471.x.

Kell DB. 2004. Metabolomics and systems biology: making sense of the soup. *Current Opinion in Microbiology* **7**:296–307 DOI 10.1016/j.mib.2004.04.012.

Kokushi E, Shintoyo A, Koyama J, Uno S. 2016. Evaluation of 2,4-dichlorophenol exposure of Japanese medaka, *Oryzias latipes*, using a metabolomics approach. *Environmental Science and Pollution Research* DOI 10.1007/s11356-016-6425-7.

Kullgren A, Samuelsson LM, Larsson DGJ, Björnsson BT, Bergman EJ. 2010. A metabolomics approach to elucidate effects of food deprivation in juvenile rainbow trout (*Oncorhynchus mykiss*). *American Journal of Physiology. Regulatory, Integrative and Comparative Physiology* **299**:R1440–R1448 DOI 10.1152/ajpregu.00281.2010.

Los DA, Murata N. 2004. Membrane fluidity and its roles in the perception of environmental signals. *Biochimica et Biophysica Acta* **1666**:142–157 DOI 10.1016/j.bbamem.2004.08.002.

Louro B, Power DM, Canario AVM. 2014. Advances in European sea bass genomics and future perspectives. *Marine Genomics* **18**:71–75 DOI 10.1016/j.margen.2014.06.010.

Luci S, Hirche F, Eder K. 2008. Fasting and caloric restriction increases mRNA concentrations of novel organic cation transporter-2 and carnitine concentrations in rat tissues. *Annals of Nutrition & Metabolism* **52**:58–67 DOI 10.1159/000118872.

Lykkesfeldt J, Svendsen O. 2007. Oxidants and antioxidants in disease: oxidative stress in farm animals. *Veterinary Journal* **173**:502–511 DOI 10.1016/j.tvjl.2006.06.005.

Médale F, Le Boucher R, Dupont-Nivet M, Quillet E, Aubin J, Panserat S. 2013. Des aliments à base de végétaux pour les Poissons d'élevage. *Productions Animales* **26**:303–316.

Mock NI, Malik MI, Stumbo PJ, Bishop WP, Mock DM. 1997. Increased urinary excretion of 3-hydroxyisovaleric acid and decreased urinary excretion of biotin are sensitive early indicators of decreased biotin status in experimental biotin deficiency. *American Journal of Clinical Nutrition* **65**:951–958.

Möder M, Löster H, Herzschuh R, Popp P. 1997. Determination of urinary acylcar-nitines by ESI-MS coupled with solid-phase microextraction (SPME). *Journal of Mass Spectrometry* **32**:1195–1204 DOI 10.1002/(SICI)1096-9888(199711)32:11<1195::AID-JMS578>3.0.CO;2-9.

Niu Q-Y, Li Z-Y, Du G-H, Qin X-M. 2016. (1)H NMR based metabolomic profiling revealed doxorubicin-induced systematic alterations in a rat model. *Journal of Pharmaceutical and Biomedical Analysis* **118**:338–348 DOI 10.1016/j.jpba.2015.10.026.

Obeid R, Awwad HM, Rabagny Y, Graeber S, Herrmann W, Geisel J. 2016. Plasma trimethylamine N-oxide concentration is associated with choline, phospholipids, and methyl metabolism. *American Journal of Clinical Nutrition* **103**:703–711 DOI 10.3945/ajcn.115.121269.

Ottinger M, Clauss K, Kuenzer C. 2016. Aquaculture: relevance, distribution, impacts and spatial assessments—a review. *Ocean & Coastal Management* **119**:244–266 DOI 10.1016/j.ocecoaman.2015.10.015.

Pamplona R, Naudí A, Gavín R, Pastrana MA, Sajnani G, Ilieva EV, Del Río JA, Portero-Otín M, Ferrer I, Requena JR. 2008. Increased oxidation, glycoxidation, and lipoxidation of brain proteins in prion disease. *Free Radical Biology & Medicine* **45**:1159–1166 DOI 10.1016/j.freeradbiomed.2008.07.009.

Reid SG, Bernier NJ, Perry SF. 1998. The adrenergic stress response in fish: control of catecholamine storage and release. *Comparative Biochemistry and Physiology Part C* **120**:1–27 DOI 10.1016/S0742-8413(98)00037-1.

Rimoldi S, Benedito-Palos L, Terova G, Pérez-Sánchez J. 2015. Wide-targeted gene expression infers tissue-specific molecular signatures of lipid metabolism in fed and fasted fish. *Reviews in Fish Biology and Fisheries* **26**:93–108 DOI 10.1007/s11160-015-9408-8.

Rodrigues PM, Silva TS, Dias J, Jessen F. 2012. Proteomics in aquaculture: applications and trends. *Journal of Proteomics* **75**:4325–4345 DOI 10.1016/j.jprot.2012.03.042.

Saera-Vila A, Calduch-Giner JA, Gómez-Requeni P, Médale F, Kaushik S, Pérez-Sánchez J. 2005. Molecular characterization of gilthead sea bream (*Sparus aurata*) lipoprotein lipase. Transcriptional regulation by season and nutritional condition in skeletal muscle and fat storage tissues. *Comparative Biochemistry and Physiology. Part B* **142**:224–232 DOI 10.1016/j.cbpb.2005.07.009.

Silva TS, Da Costa AMR, Conceição LEC, Dias JP, Rodrigues PML, Richard N. 2014. Metabolic fingerprinting of gilthead seabream (*Sparus aurata*) liver to track inter-actions between dietary factors and seasonal temperature variations. *PeerJ* **2**:e527 DOI 10.7717/peerj.527.

Smith CA, Want EJ, O'Maille G, Abagyan R, Siuzdak G. 2006. XCMS: processing mass spectrometry data for metabolite profiling using nonlinear peak alignment, match-ing, and identification. *Analytical Chemistry* **78**:779–787 DOI 10.1021/ac051437y.

Squire NL, Beranová Š, Wesdemiotis C. 1995. Tandem mass spectrometry of peptides. III—differentiation between leucine and isoleucine based on neutral losses. *Journal of Mass Spectrometry* **30**:1429–1434 DOI 10.1002/jms.1190301007.

Wang C, Qian Y, Zhang X, Chen F, Zhang Q, Li Z, Zhao M. 2016. A metabolomic study of fipronil for the anxiety-like behavior in zebrafish larvae at environmentally relevant levels. *Environmental Pollution* **211**:252–258 DOI 10.1016/j.envpol.2016.01.016.

Weissbach H, Etienne F, Hoshi T, Heinemann SH, Lowther WT, Matthews B, St John G, Nathan C, Brot N. 2002. Peptide methionine sulfoxide reductase: structure, mechanism of action, and biological function. *Archives of Biochemistry and Biophysics* **397**:172–178 DOI 10.1006/abbi.2001.2664.

Wiklund S, Johansson E, Sjöström L, Mellerowicz EJ, Edlund U, Shockcor JP, Gottfries J, Moritz T, Trygg J. 2008. Visualization of GC/TOF-MS-based metabolomics data for identification of biochemically interesting compounds using OPLS class models. *Analytical Chemistry* **80**:115–122 DOI 10.1021/ac0713510.

Wrzesinski K, R León I, Kulej K, Sprenger RR, Bjørndal B, Christensen BJ, Berge RK, Jensen ON, Rogowska-Wrzesinska A. 2013. Proteomics identifies molecular networks affected by tetradecylthioacetic acid and fish oil supplemented diets. *Journal of Proteomics* **84**:61–77 DOI 10.1016/j.jprot.2013.03.027.

Xu H-D, Wang J-S, Li M-H, Liu Y, Chen T, Jia A-Q. 2015. (1)H NMR based metabolomics approach to study the toxic effects of herbicide butachlor on goldfish (*Carassius auratus*). *Aquatic Toxicology* **159**:69–80 DOI 10.1016/j.aquatox.2014.11.020.

Xu F, Zou L, Lin Q, Ong CN. 2009. Use of liquid chromatography/tandem mass spectrometry and online databases for identification of phosphocholines and lysophosphatidylcholines in human red blood cells. *Rapid Communications in Mass Spectrometry* **23**:3243–3254 DOI 10.1002/rcm.4246.